

Periodic orbits, localization in normal mode space, and the Fermi–Pasta–Ulam problem

S. Flach^{a)}

Max-Planck-Institut für Physik komplexer Systeme, Nöthnitzer Str. 38, D-01187 Dresden, Germany

M. V. Ivanchenko

Department of Applied Mathematics, University of Leeds, Leeds, LS2 9JT, United Kingdom

O. I. Kanakov and K. G. Mishagin

Department of Radiophysics, Nizhny Novgorod University, Gagarin Avenue 23, 603950 Nizhny Novgorod, Russia

(Received 6 October 2007; accepted 10 November 2007)

The Fermi–Pasta–Ulam problem was one of the first computational experiments. It has stirred the physics community since, and resisted a simple solution for half a century. The combination of straightforward simulations, efficient computational schemes for finding periodic orbits, and analytical estimates allows us to achieve significant progress. Recent results on q -breathers, which are time-periodic solutions that are localized in the space of normal modes of a lattice and maximize the energy at a certain mode number, are discussed, together with their relation to the Fermi–Pasta–Ulam problem. The localization properties of a q -breather are characterized by intensive parameters, that is, energy densities and wave numbers. By using scaling arguments, q -breather solutions are constructed in systems of arbitrarily large size. Frequency resonances in certain regions of wave number space lead to the complete delocalization of q -breathers. The relation of these features to the Fermi–Pasta–Ulam problem are discussed. © 2008 American Association of Physics Teachers.

[DOI: 10.1119/1.2820396]

I. INTRODUCTION

The characterization of dynamical excitations of a system is one of the fundamental tasks in condensed matter physics. For quantum systems the problem is obtaining the correct description of the many-particle wave functions. For many-particle nonlinear classical systems the main difficulty is relating the excitations to families of trajectories in phase space.

Because a generic classical Hamiltonian system is non-integrable, it will evolve chaotically on large observation times for almost any initial condition. Hamiltonian chaos describes the decay of excitations on large time scales. The excitations are typically characterized by nonchaotic trajectories. Kolmogorov, Arnold, and Moser showed that regular dynamics on invariant N -dimensional tori persists in many non-integrable systems with a finite number of degrees of freedom N .¹ Especially important are the simplest realizations of low-dimensional invariant structures—periodic orbits. Periodic orbits exist even in strongly chaotic systems and can densely fill the chaotic phase space volume despite having zero measure (just like the rational numbers fill the space of real numbers). Periodic orbits are the most natural class of regular trajectories which can describe excitations. An example of such excitations are discrete breathers. They are periodic solutions of nonlinear lattice systems localized in the direct space that persist in infinite lattices.^{2–4}

Periodic orbits can be computed numerically with high accuracy for large systems. Therefore computational approaches can often help in characterizing dynamical excitations, especially when combined with analytical arguments. In the following we will show how such methods allow us to successfully study one of the most famous problems in computational and statistical physics—the Fermi–Pasta–Ulam problem.

II. THE FERMI–PASTA–ULAM PROBLEM

In 1953 Enrico Fermi, John Pasta, and Stanislaw Ulam studied the problem of energy redistribution between the linear normal modes of an anharmonic atomic chain and published the results as an internal report of the Los Alamos National Laboratory.⁵ They used one of the first available computers with modern architecture, and performed what can be called one of the first computational experiments.

The equations of motion describe N particles with a nonlinear interaction between nearest neighbors, with either quadratic (the α -FPU model)

$$\ddot{x}_n = (x_{n+1} - 2x_n + x_{n-1}) + \alpha[(x_{n+1} - x_n)^2 - (x_n - x_{n-1})^2], \quad (1)$$

or cubic terms (the β -FPU model)

$$\ddot{x}_n = (x_{n+1} - 2x_n + x_{n-1}) + \beta[(x_{n+1} - x_n)^3 - (x_n - x_{n-1})^3]. \quad (2)$$

The coordinate $x_n(t)$ corresponds to the displacement of the n th particle from its equilibrium position. The particle mass and harmonic spring constant are assumed to be one.

Fixed boundary conditions $x_0 = x_{N+1} = 0$ are used. The canonical transformation

$$x_n(t) = \sqrt{\frac{2}{N+1}} \sum_{q=1}^N Q_q(t) \sin\left(\frac{\pi q n}{N+1}\right) \quad (3)$$

diagonalizes and solves the linear problem $\alpha = \beta = 0$ using the normal mode coordinates $Q_q(t)$. The mode number $q = 1, \dots, N$ relates each of these modes to its corresponding normal mode frequency $\omega_q = 2 \sin(\pi q / 2(N+1))$. The equations of motion in normal mode space become

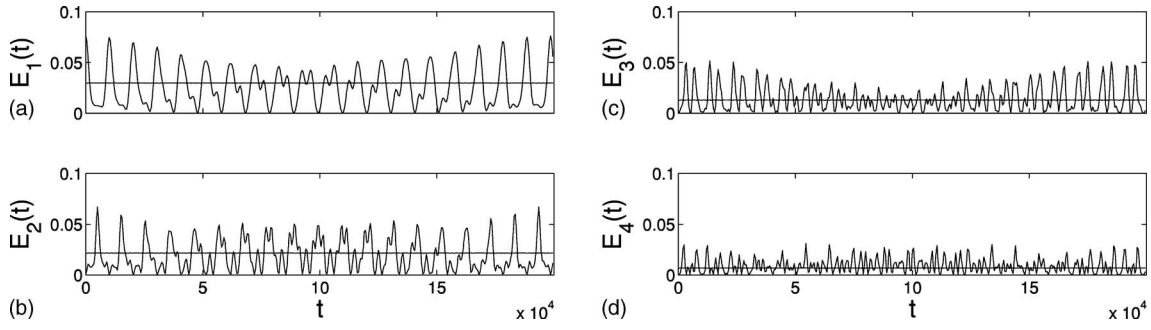


Fig. 1. The evolution of the energy of modes $q=1, 2, 3, 4$ for the FPU trajectory (oscillating curves) and the exact periodic orbit of the q -breather (horizontal lines). The parameters are $\alpha=0.25$, total energy $E=0.077$, and $N=32$ (see Ref. 13).

$$\ddot{Q}_q + \omega_q^2 Q_q = - \frac{\alpha}{\sqrt{2(N+1)}} \sum_{l,m=1}^N \omega_q \omega_l \omega_m B_{q,l,m} Q_l Q_m \quad (4)$$

for the α -FPU chain in Eq. (1) and

$$\ddot{Q}_q + \omega_q^2 Q_q = - \frac{\beta}{2(N+1)} \sum_{l,m,n=1}^N \omega_q \omega_l \omega_m \omega_n C_{q,l,m,n} Q_l Q_m Q_n \quad (5)$$

for the β -FPU chain in Eq. (2). The interaction coefficients

$$B_{q,l,m} = \sum_{\pm} (\delta_{q \pm l \pm m, 0} - \delta_{q \pm l \pm m, 2(N+1)}), \quad (6)$$

$$C_{q,l,m,n} = \sum_{\pm} (\delta_{q \pm l \pm m \pm n, 0} - \delta_{q \pm l \pm m \pm n, 2(N+1)} - \delta_{q \pm l \pm m \pm n, -2(N+1)}) \quad (7)$$

give the coupling between the modes. The coupling is nonlinear, selective, and does not have a characteristic interaction range (or distance) in normal mode space. Thus, even very distant modes in normal mode space are coupled. In the absence of this interaction there exist N integrals of motion which correspond to the energies of the normal modes $E_q = (\dot{Q}_q^2 + \omega_q^2 Q_q^2)/2$.

Fermi, Pasta, and Ulam considered the evolution of the nonlinear chain with the single mode $q_0=1$ with the lowest frequency initially excited.⁵ They used standard numerical schemes to approximate the differential equations and monitored the state of the system for times that are orders of magnitude larger than the largest periods of oscillation of the normal modes. It was expected that after some time other modes would become excited as well, and the energy would eventually be equally distributed over the entire spectrum. That was the way they anticipated a transition to thermal equilibrium. To their big surprise they observed the opposite result (see Fig. 1). The energy stayed localized in several low frequency modes for times that are orders of magnitude larger than the typical oscillation periods of these normal modes. Recurrences of almost all the energy into the initially excited mode were observed as well. Later computational studies revealed that there exist energy thresholds and system size thresholds above which equipartition was observed on relatively short time scales.^{6,7} Many questions arise. Why is the energy localized in a few modes below the thresholds?

Why does the energy spread quickly into the entire spectrum above the thresholds? How do the threshold values scale with the parameters of the system?

Figure 2 shows the mode energy density distribution $\varepsilon_q = E_q/(N+1)$ for an initial energy that is larger than the one considered in Ref. 5, but yet well below the previously mentioned thresholds. The distributions are plotted on a logarithmic scale and for times $t=10^4, 10^5$, and 10^6 . Because the mode energies are time dependent, the densities were averaged over a time interval of $\Delta t=10^4$. We observe exponential localization of the energy distribution in normal mode space, which was first noted by Galgani and Scotti.⁸ Such a distribution is formed on a very short time scale τ_1 , and possesses a core — the few modes which are strongly excited — and a tail of exponentially weakly excited modes. Also shown in Fig. 2 is a slow resonant pumping of energy from the core of the distribution into its tails for later times. This process ultimately brings the system to equipartition, but on the much larger time scale $\tau_2 \gg \tau_1$. Fermi, Pasta, and Ulam⁵ performed their numerical studies at lower energies, and therefore τ_2 was even larger in their case. If the initial energy is further increased, a threshold value may be reached for

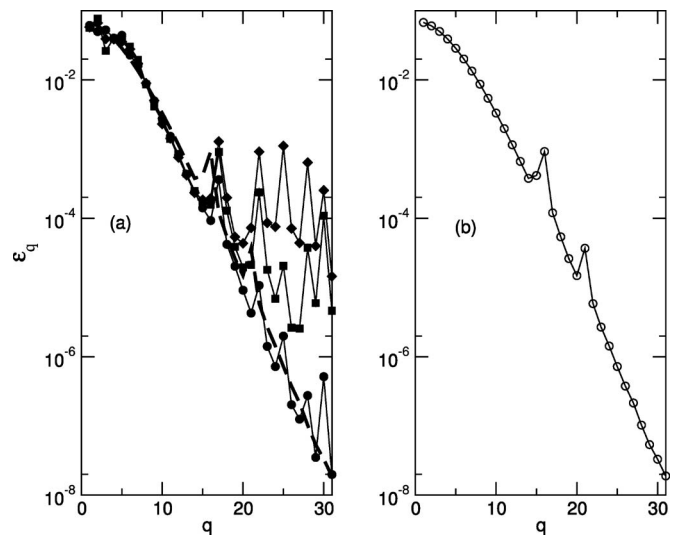


Fig. 2. (a) Distributions of the mode energy densities for the FPU trajectory with $q_0=1$, $N=31$, $\alpha=0.33$, and $E=0.32$. Circles: $t=10^4$, squares: $t=10^5$, diamonds: $t=10^6$. The dashed line is the q -breather from (b) for comparison. (b) Distributions of the mode energy densities for the q -breather with the same parameters as in (a) (see Ref. 12).

which the time scale of the core-tail pumping becomes comparable with the transition time to the exponential distribution $\tau_2 \approx \tau_1$.^{6,7} Below these threshold values the time scales differ by orders of magnitudes, and the evolution on times $\tau_1 \ll t \ll \tau_2$ corresponds to the observations of Ref. 5. Fermi, Pasta, and Ulam viewed their observations as a problem of (perhaps complete) the absence of equipartition (that is, ergodicity)—a problem now known as the FPU problem. From a contemporary perspective, the FPU problem can be reformulated as the following set of questions:

- Why are there at least two qualitatively different time scales τ_1 and τ_2 ?
- Are there low-dimensional invariant manifolds in phase space which approximate the dynamics of the FPU trajectories for times less than τ_2 ?
- Can we estimate the localization length of the exponentially localized energy distribution in normal mode space?
- Is the localization length related to the time scales?
- Does the FPU observation hold in the limit of infinite systems, as well as in two- and three-dimensional systems?

There is a long history of studies of the FPU problem,^{9–11} which, even if not directly answering all of these questions, defined new fields of research in nonlinear dynamics, chaos theory, and soliton theory.

III. PERIODIC ORBITS— q -BREATHERS

From the results of Sec. II we may conjecture that the exponentially localized state observed on the FPU trajectory is a long-lived excitation, which is destroyed after time τ_2 . Therefore (see discussion in Sec. I) we anticipate that this excitation is close to an exact periodic orbit for times $t \ll \tau_2$. Then the observed dynamics will be almost regular. Such a periodic orbit will correspond to a slightly deformed normal mode. There exists a rigorous method of constructing such a periodic orbit, starting from the linear limit $\alpha = \beta = 0$.^{13,14} In this limit the periodic orbit is given by exciting a single mode with mode number q_0 with an energy E . With these conditions we isolate a unique periodic orbit in the multi-dimensional phase space of the system.

The linear spectrum of the FPU chain obeys the non-resonance condition¹⁵

$$\omega_q \neq n\omega_{q_0} \quad (8)$$

for all integer n and $q \neq q_0$. This condition allows us to apply a theorem due to Lyapunov,¹⁶ which states that the original periodic orbit can be continued into the domain of nonzero nonlinearity for fixed energy.¹³ Continuation means that close to the periodic orbit of the linear system we will find a new periodic orbit in the phase space of the nonlinear system with identical energy E . This new periodic orbit, being a closed loop in phase space, can be viewed as a continuous deformation of the periodic orbit of the linear system, as the nonlinearity is increased.

The numerical methods of constructing q -breathers^{13,14} use the fact that a periodic orbit corresponds to a fixed point in the generalized Poincaré maps (sections) in phase space. Let us explain one of the possible realizations of such a numerical scheme in more detail.

We consider initial conditions for which all normal mode velocities $\dot{Q}_q(t=0) = 0$. Then the kinetic energy at $t=0$ is exactly zero. Note that the kinetic energy is given by the one-

half of the sum over all squared mode velocities, and the total energy is conserved during the integration. We construct a N -dimensional vector where each component is the amplitude of a given mode. This vector represents the configuration space of the system. Then we integrate the equations of motion numerically, until the velocity \dot{Q}_{q_0} crosses zero two times (because an oscillator needs two turning points to return to its initial state). At that moment we again measure all mode amplitudes, and obtain a second (final) vector. If the initial and final vectors coincide, the potential energies coincide as well. Therefore the kinetic energy at the final time will be zero, and our initial condition is located on a periodic orbit. The period of the orbit can be determined by computing the time we needed to reach the final vector.

What if the final vector does not coincide with the initial one? Then we compute the difference vector between the final and initial vectors. It will also have N components. Our task is to slightly vary the initial vector components such that all the components of the difference vector shrink to zero. In other words, we are trying to zero N functions (the components of the difference vector) by varying N variables (the components of the initial vector). Generalized Newton–Raphson methods will do the job if the initial vector is suitably close to a desired solution. Because the final vector is the outcome of a map in configurational space, we can also say that we are looking for a fixed point of that map. If we want to find a fixed point for a given total energy (or some other constraint) we have to limit the variations of the initial vector accordingly. For practical reasons it is convenient to first fix the amplitude of mode Q_{q_0} to a given value a to find the corresponding periodic orbit, calculate its energy, and then to vary a such that the desired energy value is realized.

Once a periodic orbit is obtained, we also compute its stability properties. A periodic orbit is said to be (marginally) stable if a small perturbation of the orbit in phase space does not grow in time; otherwise it is unstable. The initial smallness of the perturbation allows us to perform a linearization of the phase space flow around the periodic orbit (see Ref. 1 for details). In practice it amounts to the following procedure. Take a reference point on the periodic orbit. Consider $2N$ small perturbations in the $2N$ different directions in phase space. Integrate each of these perturbations over one period of the orbit, and obtain a new (still quite small) perturbation. The components of these final perturbations define a Floquet matrix, which maps any initial perturbation into a final one. The matrix is symplectic.¹⁷ In a nutshell, if λ is an eigenvalue of a symplectic matrix, so are $1/\lambda$, λ^* and $1/\lambda^*$. Compute the eigenvalues of that matrix. Any eigenvalue which is located on the unit circle in the complex plane corresponds to a perturbation that does not grow in time. Eigenvalues outside the unit circle correspond to perturbations which grow exponentially fast in time. Note that each eigenvalue outside the unit circle has a symmetry-related partner inside the unit circle due to the symplectic properties of the Floquet matrix. The interested reader may consult Ref. 17, where details of the ways to compute and analyze periodic orbits are discussed.

A. Results for the α -FPU model, low frequencies

The dynamics of the continued periodic orbit incorporates many normal modes, because nonlinearity induces mode-mode interactions. The numerical procedure described above

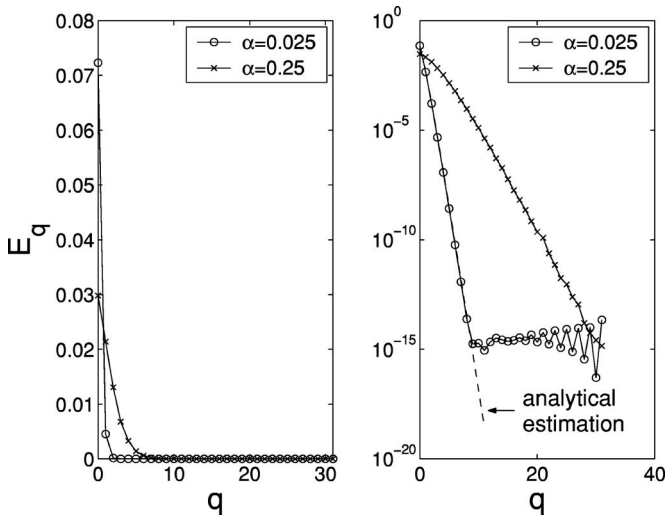


Fig. 3. Stable q -breathers for $\alpha=0.025$ and $\alpha=0.25$, $E=0.077$, $N=32$, and $q_0=1$. The dashed line is the result of Eq. (9) (see Ref. 14).

was used and new periodic orbits were found. The amplitude and energy distributions of the normal modes in such a periodic orbit turn out to be exponentially localized [see Figs. 1 and 2(b)]. We call these solutions q -breathers; they are periodic in time and localized in normal mode space. Note that the shape of the energy distribution of q -breathers is remarkably close to the one of the FPU-trajectory for $t < \tau_2$ and identical parameters (energy E and seed mode number q_0).

Any numerical evaluation should, if possible, be accompanied by analytical considerations. For q -breathers that is possible with the help of standard perturbation approaches. For the case of low frequency modes the energy distribution in the q -breather has been estimated to be¹⁴

$$E_{q=nq_0} = \gamma^{n-1} n^2 E_{q_0}, \quad \sqrt{\gamma} = \frac{\alpha \sqrt{E_{q_0}} (N+1)^{3/2}}{\pi^2 q_0^2}. \quad (9)$$

The q -breathers are localized in normal mode space if mode energies shrink with increasing distance from q_0 . From Eq. (9) it follows that q -breathers are exponentially localized if $\gamma < 1$: $E_q \sim e^{-q/\xi}$, where ξ is the localization length. For $\gamma=1$ Eq. (9) predicts the parameter values for which a q -breather delocalizes. If this condition is reached upon variation of a parameter, we say that a delocalization threshold has been reached. If we vary a second parameter, we can keep γ unchanged. In this way we can vary all parameters, keep γ constant, and obtain scaling relations between all the parameters. The inverse localization length ξ^{-1} is proportional to $q_0^{-1} \ln \gamma$. When $\gamma=1$ the q -breather delocalizes, which implies $\tau_2 \approx \tau_1$. These are, among many others, predictions which can be tested by comparing to q -breather solutions and FPU trajectories, which are obtained using the previously described computational methods.

The numerical results and the estimate in Eq. (9) are shown in Fig. 3. The q -breather solutions are linearly stable.^{13,14} The agreement between the computations and theory is very good, especially for strongly localized energy profiles.

Note that in real space the energy distributions are delocalized both for the FPU and for the q -breather trajectories, and do not show remarkable features.^{13,14}

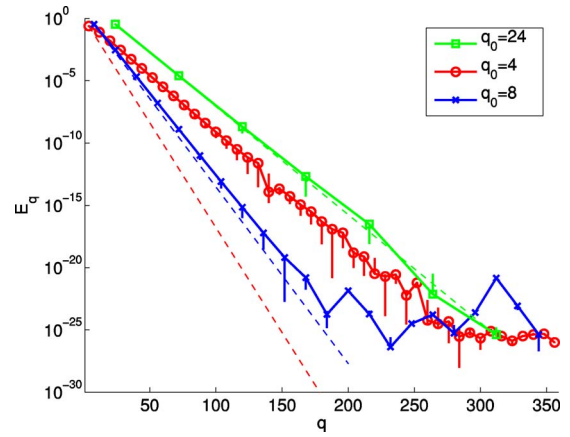


Fig. 4. (Color online) The profiles of the q -breather solutions for $N=359$, $\beta=1$, $E=0.346$, and $q_0=4, 8$, and 24 . The symbols denote the mode energies at the time when the coordinates $x_n(t)=0$. The vertical bars denote the range of mode energy values realized during one period of the q -breather. The dashed lines are the result if Eq. (10) with $q_0=24, 8$, and 4 from top to bottom (see Ref. 21).

B. Results for β -FPU, low frequencies

If we apply the perturbation methods we have mentioned to the β -FPU problem, we arrive at the result for the energy distribution in the q -breather:¹⁴

$$E_{q=(2n+1)q_0} = \lambda^n E_{q_0}, \quad \sqrt{\lambda} = \frac{3\beta E_{q_0} (N+1)}{8\pi^2 q_0^2}. \quad (10)$$

The necessary condition for the localization of the q -breather is $\lambda < 1$. The inverse localization length ξ^{-1} is proportional to $(2q_0)^{-1} \ln \lambda$. If $\lambda=1$, the q -breather delocalizes, and thus we expect that $\tau_2 \approx \tau_1$. The numerical and analytical results (10) are presented in Fig. 4. For $q_0=4$ the asymptotic result for λ fails, although the exponential profile of the mode energies still holds.

The q -breathers become unstable if $6\beta E(N+1)/\pi^2 > 1$,¹⁴ but as long as they remain strongly localized, the FPU trajectories do not delocalize quickly.¹⁸ Remarkably the FPU trajectory shows a change from regular to weakly chaotic dynamics in its core when increasing the initial energy E above a certain value.¹⁸ This value corresponds to the condition for changing the stability of the q -breather. It is well known that for non-integrable Hamiltonian systems, chaotic trajectories appear close to an unstable periodic orbit.¹⁹

Why does the instability of the q -breather, and the chaotic dynamics close to it, not destroy the exponential localization of the mode energy profile? The answer might be that a q -breather which is well localized in normal mode space does not allow for a resonant interaction between core and tail modes, because if such a resonance was present, it would lead to a delocalization of the periodic orbit itself. Instabilities in the core of the distribution, that is, resonances between modes inside the core, are what is left. They can lead to a chaotic dynamics inside the core, but not to a delocalization, due to the absence of resonances between the core and the tail modes.

C. Results for high frequencies

Localization is observed also for high frequency seed modes. In Fig. 5 the energy distributions for the FPU and

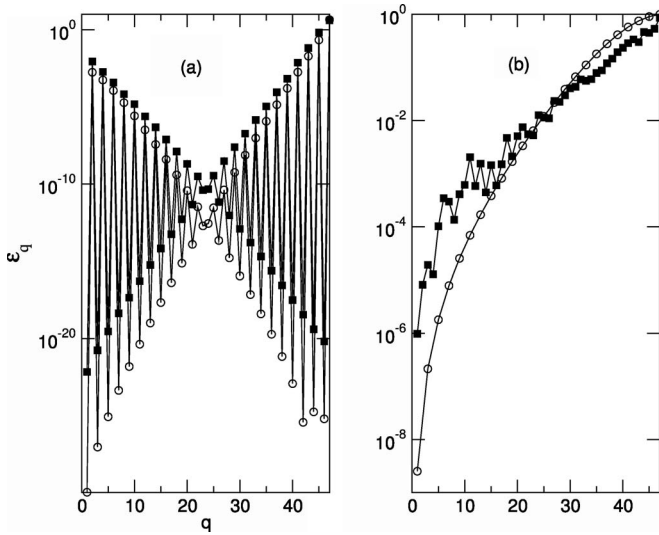


Fig. 5. Energy density distribution for the FPU trajectory (squares, $t=10^5$) and q -breather (circles) for $N=47$, $E=4.7$, and $q_0=47$. (a) $\alpha=0.25$ and (b) $\beta=0.25$ (see Ref. 12).

q -breather trajectories are shown.¹² The only difference from low frequencies is that for the α -FPU model high and low frequency modes become excited in pairs, in agreement with the predictions of perturbation theory.¹²

IV. GENERALIZATION TO TWO AND THREE DIMENSIONS

The condition for applying Lyapunov's theorem to the continuation of a q breather is the absence of resonances [see Eq. (8)]. A finite system has a discrete spectrum and thus Lyapunov's theorem is applicable. A generalization of the results in Sec. III has been performed by considering finite lattices with spatial dimensions $d=2$ and 3. Instead of mode numbers we now have mode vectors with d integer components. The main properties of the solutions for q -breather solutions do not change.²⁰ In Fig. 6 an example of a q -breather solution in $d=2$ is shown.

For the β -FPU model we can generalize the perturbation theory and predict the energy distribution²⁰

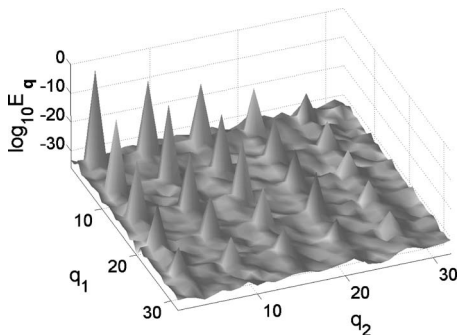


Fig. 6. Mode energy distributions for a q -breather in a two-dimensional FPU lattice with $N=32 \times 32$, $E=1.5$, $\mathbf{q}_0=(3,3)$, and $\beta=0.5$ (see Ref. 20).

$$E_{(2n+1)\mathbf{q}_0} = \lambda_d^{2n} E_{\mathbf{q}_0}, \quad \lambda_d = \frac{3\beta E_{\mathbf{q}_0} (N+1)^{2-d}}{2^{2+d} \pi^2 |\mathbf{q}_0|^2}. \quad (11)$$

The numerically computed q -breather solutions show quantitative agreement with these estimates.²⁰

V. SCALING AND TRANSITION TO MACROSCOPIC SYSTEMS

The perturbation theory results in Eqs. (9)–(11) show that after replacing the extensive parameters (the energy E and the mode number q) by intensive ones (the energy density $\varepsilon=E/(N+1)$ and wave number $k=\pi q/(N+1)$), the localization length becomes independent of the system size N . Consequently, we expect that q -breathers will persist in the limit of an infinitely large macroscopic system. Consider a q -breather solution $Q_q(t)$ for a finite chain of size N and another chain of size $\tilde{N}+1=r(N+1)$, where $r=2,3,4,\dots$. It follows that

$$\tilde{Q}_{\tilde{q}}(t) = \begin{cases} \sqrt{r} Q_q(t), & \tilde{q} = rq \\ 0, & \tilde{q} \neq rq \end{cases} \quad (12)$$

is a solution for the larger chain.²¹

By increasing r to infinity we will obtain solutions for infinitely large macroscopic systems. The scaling procedure is easily generalized to $d=2$ and 3 as well as to free and periodic boundary conditions.²¹

Suppose that q -breathers exist in an infinitely large chain. Then Eq. (10) with k and ε instead of q and E gives

$$\ln \varepsilon_k = \left(\frac{k}{k_0} - 1 \right) \ln \sqrt{\lambda} + \ln \varepsilon_{k_0}, \quad \sqrt{\lambda} = \frac{3\beta \varepsilon_{k_0}}{8 k_0^2}. \quad (13)$$

We see that the analytical result for the mode energy profile is independent of system size if intensive parameters are used.

Consider a finite chain with initial length $N_0=15$ and seed wave number $\bar{k}_0=\pi/15$. We increase the system size and numerically compute q -breather solutions for the seed mode number q_0 which is the closest to $\bar{k}_0(N+1)/\pi$. The solution is then used to approximate the coefficient λ by the ratio $\varepsilon_{5q_0}/\varepsilon_{3q_0}$ [see Fig. 7(a)]. The results confirm the independence of the approximate value of λ if $N+1=r(N_0+1)$. For other values of N we probe λ with different seed wave numbers k_0 in the vicinity of \bar{k}_0 . The continuous behavior of $\lambda(k_0)$ [see Fig. 7(b)], irrespective of system size N , confirms these conclusions for macroscopic systems.

If the energy density ε is fixed to a given value, it follows from the geometric series in Eq. (10) that $\varepsilon_{k_0}=(1-\lambda)\varepsilon$. We use Eq. (13) and calculate the slope S of the energy density distribution (on a logarithmic scale):²¹

$$S = \frac{1}{k_0} \ln \sqrt{\lambda}, \quad \sqrt{\lambda} = \frac{\sqrt{1+4\nu^4/k_0^4}-1}{2\nu^2/k_0^2}, \quad \nu^2 = \frac{3\beta}{8} \varepsilon. \quad (14)$$

The absolute value of S equals the inverse localization length $\xi^{-1}=|S|$. The slope S depends on the seed wave number k_0 and on the effective nonlinearity parameter ν , which is determined by the product of the energy density ε and the nonlinearity strength β . The localization length diverges if $k_0 \rightarrow 0$ and takes a minimum value of $\xi_{\min} \approx \nu/0.7432$ at k_0

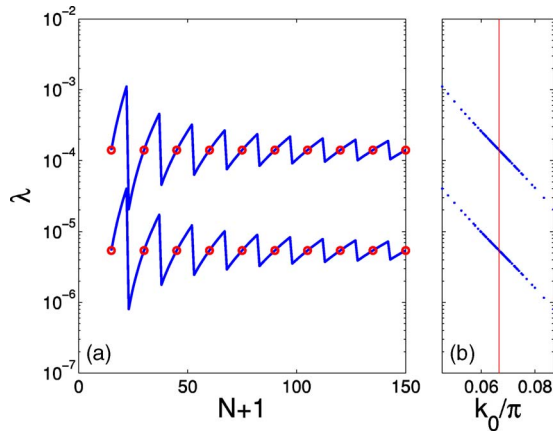


Fig. 7. (a) Dependence of λ on the size of the chain for the q -breather with energy density $\varepsilon=4 \times 10^{-4}$ (lower curve) and 2×10^{-3} (upper curve) and $\beta=1$. The open circles correspond to $N+1=r(N_0+1)$ with $N_0=15$, where r is an integer. (b) The dependence of λ on the wave number k_0 for the corresponding data from (a) (see Ref. 21).

$=k_{\min} \approx 2.577\nu$.²¹ The localization length for $k_0=k_{\min}$ also increases for increasing ν . In the limit $k_0 \gg \nu$ we estimate $S \approx -2/k_0 \ln(k_0/\nu)$, and for $k_0 \ll \nu$ we obtain $S \approx -k_0/(2\nu^2)$.²¹ It follows that for a given energy density there exists a seed wave number k_{\min} for which the q -breather is most strongly localized. Moreover, q -breathers tend to delocalize for $k_0 \ll k_{\min}$, that is, in the limit of long wavelength. These analytical predictions may now be compared to careful numerical computations of q -breathers.

The analytical and numerical results are compared in Fig. 8. The numerical results confirm that the localization length does not depend on the system size. We also observe the minimum $S(k_0)$ whose depth and location vary with the energy as expected. A systematic mismatch between the theory and the numerical results for small k_0 is caused by higher order corrections to the perturbation theory. The q -breathers from Fig. 4 for $q_0=4, 8$ and 24 correspond to the most left symbol on the middle curve in Fig. 8, the minimum on that curve, and a point to the right of it, respectively.

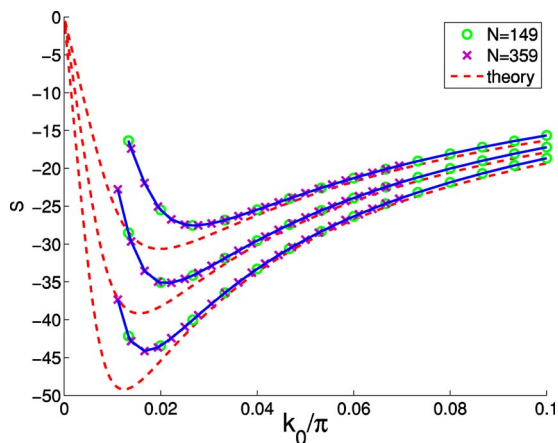


Fig. 8. The slope $S(k_0)$ for $\beta=1$ and $\varepsilon=1.57 \times 10^{-3}$, 9.6×10^{-4} , and 6.08×10^{-4} (dashed lines from top to bottom). The symbols and connecting lines are the results of the numerical solutions of q -breathers for $N=149$ and $N=359$ (see Ref. 21).

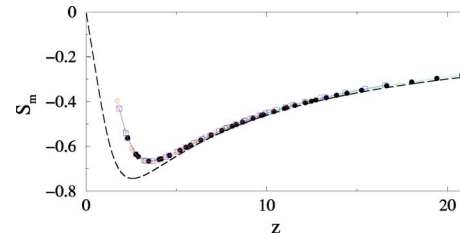


Fig. 9. $S_m(z)$ (dashed line) with $z=k_0/\nu$. The symbols and connecting lines are the rescaled data from the numerical q -breather solutions in Fig. 8 (see Ref. 21).

It follows from Eq. (14) that the quantity $S_m(z)=\nu S$ depends on a single variable, namely the dimensionless seed wave number $z=k_0/\nu$. It implies that knowing this single master slope function is sufficient to predict the localization property of any q -breather, at any energy, any seed wave number, etc. In Fig. 9 the dependence of $S_m(z)$ is shown together with the rescaled numerical data from Fig. 8.

Despite the systematic mismatch between the numerical data and the theoretical prediction for small $z=k_0/\pi$, the scaled numerical data collapse to a single curve. Therefore, the theoretically predicted scaling law in Eq. (14) is well confirmed. Analogous results have been obtained for the α -FPU model, and for both FPU models for seed wave numbers with frequencies near the upper edge of the spectrum ω_q .

VI. DISCUSSION

The reason for the delocalization of q -breathers at the edges of the linear spectrum are resonances between normal mode frequencies: $\omega_{q_0} \approx n\omega_{nq_0}$ for low frequency modes and $\omega_{q_0} \approx \omega_q$ for high frequency modes. Thus it is expected that the excited mode with a wave number close to an edge of the spectrum will decay into many other modes, and the two time scales $\tau_2 \approx \tau_1$. These time scales must diverge in the limit of small frequencies, due to conservation of total mechanical momentum. Hence the time scale τ_{sim} of the simulation is important. Suppose we excite a normal mode that is close to a well-localized q -breather when $\tau_2 \gg \tau_1$. If $\tau_{\text{sim}} < \tau_2$, the excitation of this normal mode will quickly spread into a packet, but stay localized in normal mode space for all observation times (this localization is the FPU problem). If $\tau_{\text{sim}} > \tau_2$, the long time of nonequipartition will be eventually replaced by a thermalized state.

Suppose we excite a low frequency normal mode for which the corresponding q -breather is delocalized, and $\tau_2 \approx \tau_1$. If $\tau_{\text{sim}} < \tau_2$, the normal mode will not decay at all during the observation time. The simulation will thus recover the linear dynamics of the bare modes as if the nonlinearity were absent. If $\tau_{\text{sim}} > \tau_2$, the normal mode will begin to decay into other modes, but there will be no intermediate state in which only a few other modes become excited; rather the entire available mode space will be excited at once. That means that these low frequency modes will behave like linear modes for short times and fully chaotically for larger times, without any intermediate regime of exciting only a few other modes.

The normal mode frequencies ω_q are periodic in the wave number k . That period defines the irreducible part of the wave number space, which therefore has finite width (for the

chain it is π). Localization in wave number space is meaningful only when the localization length $\xi < \pi$. Thus, from our previous results we conclude that all q -breathers which are closer than some critical distance Δk_0 of the seed wave number k_0 from the spectrum edge delocalize. For non-zero $\nu^2 \sim \beta \varepsilon$ $\Delta k_0 \neq 0$. Thus, there exists a range of k_0 for which the excitation of the normal mode decays and the normal mode picture may become ill defined. The range Δk_0 is an increasing function of ν , and for some critical value $\nu \Delta k_0 \approx \pi$, which means that normal modes do not characterize the dynamics of the system. That corresponds to the regime of strong interaction between modes. For small ν this strong interaction occurs near the edges of the spectrum only.

Let us discuss the results for finite systems. A given ν corresponds to a finite Δk_0 . A finite system implies a discrete set of wave numbers for the normal modes. The thermal conductivity of anharmonic acoustic lattices is governed by the dynamics of low frequency waves. To numerically observe a conductivity different from the free propagating (ballistic) one, we have to resolve the regime of strong interactions. In particular, we have to choose a system size greater than $N_c \sim 1/(\Delta k_0)$. The theory we have presented allows us to obtain relevant quantitative estimates, and the computational results show that these considerations are valid.

Finally, let us discuss the resonance peaks in the tails of the distributions in Fig. 2, which are observed in the FPU trajectory and also in the q -breather. A quantitative explanation of the origin and position of these peaks was given recently.¹² They are generated by the closeness to the resonance in Eq. (8) for certain mode numbers. It is easy to check that the peaks appear in the upper half of the frequency spectrum and for low frequency seed modes only. To explain the appearance of these peaks we have to consider the dispersion relation more accurately.¹² Numerical experiments show that these resonant peaks trigger the transition to equipartition in the FPU trajectory.¹² The nature of the pathway to equipartition for high frequency seed modes, for which these peaks are absent, remains a puzzle.

There are many other questions that still wait for answers. We have to explore other nonlinear models and test which of the results we have discussed will be generic and which not. We need to obtain reliable estimates on the dependence of $\tau_{1,2}$ on the parameters and compare with the results for q -breathers. We have to determine whether q -breather-like excitations are spontaneously generated at thermal equilibrium and to characterize their statistical properties. This list could be continued, but there must be an end to everything, and our story finishes here.

ACKNOWLEDGMENTS

The authors thank D. Bambusi, A. Lichtenberg, L. Galgani, T. Penati and A. Ponno for useful discussions. M.I., O.K. and K.M. acknowledge support from RFBR, Grant No. 07-02-01404.

^{a)}Electronic mail: flach@mpipks-dresden.mpg.de

¹V. I. Arnold, *Mathematical Methods of Classical Mechanics* (Springer-Verlag, New York, 1989).

²D. K. Campbell, S. Flach, and Yu. S. Kivshar, "Localizing energy through nonlinearity and discreteness," *Phys. Today* **57**(1), 43–49 (2004).

³S. Flach and C. R. Willis, "Discrete breathers," *Phys. Rep.* **295**, 182–264 (1998).

⁴S. Flach and A. Gorbach, "Discrete breathers in Fermi-Pasta-Ulam lattices," *Chaos* **15**, 015112-1–10 (2005).

⁵E. Fermi, J. Pasta, and S. Ulam, Los Alamos Report LA-1940 (1955), Also published in *Collected Papers of Enrico Fermi*, edited by E. Segré (University of Chicago Press, Chicago, 1965).

⁶D. L. Shepelyansky, "Low-energy chaos in the Fermi-Pasta-Ulam problem," *Nonlinearity* **10**, 1331–1338 (1997).

⁷L. Berchialla, A. Giorgilli, and S. Paleari, "Exponentially long times to equipartition in the thermodynamic limit," *Phys. Lett. A* **321**, 167–172 (2004).

⁸L. Galgani and A. Scotti, "Planck-like distributions in classical nonlinear mechanics," *Phys. Rev. Lett.* **72**, 1173–1176 (1972).

⁹N. J. Zabusky and M. D. Kruskal, "Interaction of solitons in a collisionless plasma and recurrence of initial states," *Phys. Rev. Lett.* **15**, 240–243 (1965).

¹⁰F. M. Izrailev and B. V. Chirikov, "Statistical properties of a non-linear chain," *Sov. Phys. Dokl.* **11**, 30 (1966).

¹¹J. Ford, "The Fermi-Pasta-Ulam problem: Paradox turns discovery," *Phys. Rep.* **213**, 271–310 (1992).

¹²T. Penati and S. Flach, "Tail resonances of FPU q -breathers and their impact on the pathway to equipartition," *Chaos* **17**, 023102-1–16 (2007).

¹³S. Flach, M. V. Ivanchenko, and O. I. Kanakov, " q -breathers in Fermi-Pasta-Ulam chains: Existence, localization and stability," *Phys. Rev. E* **73**, 036618-1–14 (2006).

¹⁴S. Flach, M. V. Ivanchenko, and O. I. Kanakov, " q -breathers and the Fermi-Pasta-Ulam problem," *Phys. Rev. Lett.* **95**, 064102-1–4 (2005).

¹⁵J. H. Conway and A. J. Jones, "Trigonometric diophantine equations (on vanishing sums of roots of unity)," *Acta Arith.* **XXX**, 229–240 (1976).

¹⁶M. A. Lyapunov, *The General Problem of Stability of Motion* (Taylor & Francis, London, 1992).

¹⁷S. Flach, "Computational studies of discrete breathers," in *Energy Localization and Transfer*, edited by T. Dauxois, A. Litvak-Hinenzon, R. S. MacKay, and A. Spanoudaki (World Scientific, Singapore, 2004), pp. 1–71.

¹⁸J. De Luca, A. J. Lichtenberg, and M. A. Lieberman, "Time scale to ergodicity in the Fermi-Pasta-Ulam problem," *Chaos* **5**, 283–297 (1995).

¹⁹A. J. Lichtenberg and M. A. Lieberman, *Regular and Chaotic Dynamics* (Springer, Berlin, 1992).

²⁰M. V. Ivanchenko, O. I. Kanakov, K. G. Mishagin, and S. Flach, " q -breathers in finite two- and three-dimensional nonlinear acoustic lattices," *Phys. Rev. Lett.* **97**, 025505-1–4 (2006).

²¹O. I. Kanakov, S. Flach, M. V. Ivanchenko, and K. G. Mishagin, "Scaling properties of q -breathers in nonlinear acoustic lattices," *Phys. Lett. A* **365**, 416–420 (2007).